

# Cholesterol efflux via HDL resecreion occurs when cholesterol transport out of the lysosome is impaired<sup>S</sup>

Tamara A. Pagler,<sup>1</sup> Angelika Neuhofer,<sup>1</sup> Hildegard Laggner, Wolfgang Strobl, and Herbert Stangl<sup>2</sup>

Center for Physiology and Pathophysiology, Department of Medical Chemistry, Medical University of Vienna, A-1090 Vienna, Austria

**Abstract** Recently, we showed that holo HDL particle uptake and resecreion occur in physiologically relevant cell lines and that HDL uptake is mediated by scavenger receptor class B type I (SR-BI). Furthermore, we established that HDL resecreion is accompanied by [<sup>3</sup>H]cholesterol efflux. This study shows that HDL uptake and resecreion occur even when LDL uptake and cholesterol trafficking are disturbed. First, we used a set of inhibitors that block cholesterol transport out of the lysosome: chloroquine, imipramine, U18666A, and monensin. In all cases, HDL retroendocytosis occurred and HDL resecreion mediated [<sup>3</sup>H]cholesterol efflux, although to a lesser extent. Second, cell lines carrying somatic mutations in intracellular cholesterol transport were used: CHO 2-2 and CHO 3-6 cells accumulated LDL-derived lipid in the lysosome but showed all components of HDL retroendocytosis. SR-BI overexpression increased HDL uptake and resecreion and [<sup>3</sup>H]cholesterol efflux in these mutant cells. Finally, we used Niemann-Pick type C (NPC) patient fibroblast cells, which carry a defect in cholesterol transfer out of the lysosome. NPC fibroblast cells accumulate cholesterol in the lysosome as a result of a mutation in the NPC1 gene. Despite disturbed intracellular cholesterol transfer, NPC fibroblast cells exhibited HDL retroendocytosis and [<sup>3</sup>H]cholesterol efflux via HDL resecreion, although to a lesser extent. Thus, [<sup>3</sup>H]cholesterol efflux via HDL resecreion is independent of the cholesterol uptake pathway via the LDL receptor and may be an alternative way to remove excess cholesterol.—Pagler, T. A., A. Neuhofer, H. Laggner, W. Strobl, and H. Stangl. **Cholesterol efflux via HDL resecreion occurs when cholesterol transport out of the lysosome is impaired.** *J. Lipid Res.* 2007. 48: 2141–2150.

**Supplementary key words** scavenger receptor class B type I • high density lipoprotein • endocytosis • Niemann-Pick type C

HDL plays a major role in reverse cholesterol transport, by which excess cholesterol is transported from the periphery back to the liver for disposal. It is believed that reverse cholesterol transport plays an important role in the antiatherogenic effect of HDL. Cholesterol efflux from peripheral cells to HDL is the initial step of the reverse

cholesterol transport pathway. Several mechanisms for cholesterol efflux have been described in detail, such as cell surface cholesterol efflux to nascent and mature HDL (1). Recently, we demonstrated that HDL retroendocytosis can be associated with cholesterol efflux (2). HDL uptake, visualized by single-dye tracing (3), and resecreion occurred in hepatocytes, macrophages, and adrenocortical cells (2). HDL uptake was facilitated by the scavenger receptor class B type I (SR-BI) (2). However, the relevance of HDL uptake and resecreion for cholesterol homeostasis in cells and tissues needs to be established.

HDL retroendocytosis was first described in aortic smooth muscle cells by Bierman, Stein, and Stein (4). Ten years later, Schmitz et al. (5) described the uptake and subsequent resecreion of entire HDL particles in macrophages using electron microscopy. DeLamatre et al. (6) demonstrated retroendocytosis of iodinated HDL particles in a rat liver cell line. Moreover, Silver et al. (7) described a connection of HDL uptake with SR-BI mediating selective cholesteryl ester uptake, a process by which HDL delivers its lipid load to cells without concomitant protein degradation. The transfer of lipid from HDL to polarized hepatocytes was accompanied by a transport of the HDL particle to the endosomal recycling compartment (7). These data are in contrast to recent findings of Nieland et al. (8), who reported that HDL endocytosis is not required for selective lipid uptake by SR-BI. In addition, Wustner et al. (9) demonstrated that HDL particles were taken up by polarized HepG2 cells but that their cholesterol content arrived earlier at the apical membrane and the biliary canaliculi than the protein moiety at the endosomal recycling compartment.

Whereas little and controversial data are available on HDL particle uptake, LDL uptake via receptor-mediated endocytosis and the subsequent cholesterol delivery to the

Abbreviations: apoB, apolipoprotein B; ER, endoplasmic reticulum; FCS, fetal calf serum; NPC, Niemann-Pick type C; SR-BI, scavenger receptor class B type I.

<sup>1</sup>T. A. Pagler and A. Neuhofer contributed equally to this work.

<sup>2</sup>To whom correspondence should be addressed.

e-mail: herbert.stangl@meduniwien.ac.at

<sup>S</sup>The online version of this article (available at <http://www.jlr.org>) contains supplementary data in the form of 4 movies.

Manuscript received 31 January 2007 and in revised form 15 June 2007.

Published, *JLR Papers in Press*, July 9, 2007.

DOI 10.1194/jlr.M700056-JLR200

Copyright © 2007 by the American Society for Biochemistry and Molecular Biology, Inc.

This article is available online at <http://www.jlr.org>

endoplasmic reticulum (ER) are well established. Several naturally occurring defects in this pathway are known to lead to an accumulation of LDL-derived cholesterol in lysosomes (10). Despite the disturbance in this cholesterol uptake pathway, cells and tissues are able to maintain their cellular cholesterol content via increased synthesis of cholesterol or uptake by other mechanisms. Niemann-Pick type C (NPC) disease is one of the genetic disorders characterized by a failure to release unesterified cholesterol from lysosomes or late endosomes. NPC cells acquire apolipoprotein B/E (apoB/E)-containing lipoprotein particles through receptor-mediated endocytosis (10, 11), thereby accumulating cholesterol within acidic compartments. Lipids like sterol, sphingomyelin, and glycolipids accumulate in cells throughout the body and cause hepatosplenomegaly and progressive central nervous system degeneration (12). In NPC1<sup>+/+</sup> and NPC1<sup>+/-</sup> human fibroblasts, ABCA1 mRNA and protein levels increased in response to cholesterol loading (13). In NPC1<sup>-/-</sup> fibroblasts, however, basal ABCA1 expression was low and did not increase in response to cholesterol loading (13). These findings indicate that in addition to intracellular cholesterol traffic, cholesterol efflux to lipid-free/poor apoA-I is impaired. Other cholesterol efflux pathways, such as SR-BI-mediated cholesterol efflux, may become important in these cells. SR-BI shows the unique ability to either promote cholesteryl ester uptake or remove excess cholesterol from cells. Both contribute to its atheroprotective properties. SR-BI-mediated free cholesterol efflux is complex, as SR-BI mediates net cholesterol efflux (14, 15), bidirectional cholesterol flux to HDL (16–18), and also efflux of cholesterol to apoE phospholipid particles (19; for review, see Ref. 20). Our earlier data demonstrate that HDL uptake and resecretion mediated by SR-BI provide an alternative form of cellular cholesterol efflux (2). Here, we hypothesize that cholesterol efflux mediated by HDL resecretion may be important in cells with disturbed cholesterol efflux, in which HDL might serve as the central cholesterol-distributing platform.

Recently, we observed that HDL uptake and resecretion still occur when LDL receptor-mediated cholesterol uptake is blocked by chloroquine, a weak base that increases the intracellular pH and thereby inactivates lysosomal/acid cholesteryl ester hydrolase/lipase (21). This leads to an accumulation of LDL in the lysosome. Chloroquine does not inhibit selective cholesteryl ester uptake from HDL (2), but it completely blocks transport of the cholesterol moiety derived by selective cholesteryl ester uptake to the ER (15). Chloroquine affects several pathways and all enzymes/proteins requiring a low pH. In this study, we used several more specific inhibitors of the cholesterol uptake/transport pathway: imipramine and U18666A are two hydrophobic amines that block intracellular cholesterol transport. Imipramine was described to block cholesterol transfer out of the lysosome, whereas U18666A blocks transport from the lysosome as well as from the plasma membrane to the ER (22). Monensin is a monovalent carboxylic ionophor that disrupts ion gradients, thus preventing pH gradient formation (23). It inhibits the endocytosis of LDL through

coated pits (24) and disrupts the transit of membrane vesicles from the Golgi apparatus to the plasma membrane (25, 26). In this work, we show that even in the presence of these inhibitors, HDL retroendocytosis is still functional and [<sup>3</sup>H]cholesterol efflux mediated by HDL resecretion proceeds. We further present evidence that retroendocytosis-mediated [<sup>3</sup>H]cholesterol efflux occurs in CHO cell lines carrying a somatic mutation that traps LDL in lysosomes and that this cholesterol efflux is enhanced by SR-BI overexpression. Moreover, we show that HDL uptake and resecretion still occur even in the severe lipid-storage disorder NPC, in which cholesterol taken up by the cell is trapped in an endosomal/lysosomal compartment. Finally, we demonstrate that endocytosed HDL can remove [<sup>3</sup>H]cholesterol from NPC fibroblasts, which accumulate cholesterol taken up via the LDL receptor in the lysosome.

## METHODS

### Cell lines

For all CHO cell lines, a basal medium consisting of a 1:1 mixture of DMEM and Ham's F12 medium (Gibco) (medium A) with 100 U/ml penicillin and 100 µg/ml streptomycin was used. All cells were kept in an incubator at 37°C with 95% humidified air and 5% CO<sub>2</sub>. For the IdIA7 cell line, a CHO cell line that lacks LDL receptor activity (27), medium A with 5% fetal calf serum (FCS) was used. The IdIA7-SRBI cell line, expressing high levels of mSR-BI (15, 28), was maintained in medium A with 5% FCS and 1% geneticin (Gibco). CHO 2-2 and 3-6 cells (kindly provided by Dr. Laura Liscum) were grown with the addition of 5% FCS. Cells were transformed with mSR-BI, and clones expressing high amounts of SR-BI are termed CHO 2-2 SRBI and CHO 3-6 SRBI. These SR-BI-overexpressing cells were kept with an addition of 1% geneticin (Gibco). Primary fibroblasts, obtained from a male patient homozygous for NPC disease (kindly provided by Dr. Peter Pentchev), were kept in DMEM (high glucose) with 10% FCS, 100 U/ml penicillin, 100 µg/ml streptomycin, 1× nonessential amino acids (Sigma), 2 mM glutamine, and 1 mM sodium pyruvate.

### Lipoprotein preparation, labeling, and analysis

Plasma was collected from healthy volunteers, and lipoproteins were recovered by serial ultracentrifugation steps: LDL at a density of 1.019 g/ml and HDL at a density of 1.21 g/ml (29). Lipoproteins were iodinated with sodium <sup>125</sup>I (Hartmann Analytic, Braunschweig, Germany) using the Pierce Iodo-beads iodination reagent kit (Pierce, Rockford, IL). Usually, a specific activity of iodinated lipoprotein particles between 3,000 and 4,000 cpm/ng was obtained, and these particles were diluted with unlabeled lipoprotein to a specific activity of ~300 cpm/ng for the experiments. For fluorescence imaging, the apolipoprotein part of HDL was covalently labeled with Alexa-647 (Molecular Probes, Eugene, OR) according to the manufacturer's description.

### Retroendocytosis setup

Retroendocytosis was studied as described by DeLamatre et al. (6) with modifications as reported previously (2).

### Association experiments

On the experimental day, cholesterol-depleted cells were incubated in medium A with 2 mg/ml fatty acid-free BSA and

10  $\mu\text{g}/\text{ml}$   $^{125}\text{I}$ -HDL at  $37^\circ\text{C}$ . Unspecific binding was estimated by incubating the cells with a  $40\times$  excess of unlabeled lipoprotein. After 1 h, the medium was recovered, cells were washed twice with 50 mM Tris-HCl, pH 7.4, 0.9% NaCl, and 2 mg/ml BSA (buffer A) and twice with buffer A without BSA, and lysed using 0.1 M NaOH, and cell protein was estimated using the Bradford reagent (Bio-Rad). The radioactivity associated with lysate and medium was analyzed using a Cobra II  $\gamma$  Counter (Perkin-Elmer). Specific cell association is calculated in ng lipoprotein/mg cell protein by subtracting unspecific binding.

### Displacement experiments

In parallel, after incubation with the iodinated lipoprotein for 1 h, cells were washed twice with PBS and incubated for another 2 h at  $0^\circ\text{C}$  in medium with 2 mg/ml BSA and a  $100\times$  excess of unlabeled lipoproteins to replace surface-bound  $^{125}\text{I}$ -labeled lipoproteins. Cells were washed four times, lysed, and analyzed as described above. Specific lipoprotein uptake was estimated in cell lysate and medium.

### Chase experiments

Another parallel set of plates was washed after the  $0^\circ\text{C}$  incubation and kept for another 30 min in medium containing a  $20\times$  excess of unlabeled lipoprotein at  $37^\circ\text{C}$ . Medium was recovered. Cells were washed and lysed. Medium and cell lysate were analyzed for their content of radiolabel and were expressed as specific lipoprotein release.

### Cholesterol efflux studies

On the day before the experiment, the cellular cholesterol pool was trace-labeled with [ $^3\text{H}$ ]cholesterol (2  $\mu\text{Ci}$ ; Amersham Bioscience). The next day, cells were washed with PBS, incubated with HDL, and analyzed as described for the retroendocytosis setup. Medium and lysates from cells labeled with [ $^3\text{H}$ ]cholesterol were analyzed directly by scintillation counting.

### Inhibitor treatment

In the case of treatment with chloroquine, imipramine, U18666A, or monensin (Sigma), cells were preincubated for 15 min with the inhibitor before the addition of  $^{125}\text{I}$ -HDL. The experiment was continued as described above.

### Cholesterol esterification

On the day of the experiment, cells were washed three times with PBS and incubated in DMEM containing 2 mg/ml fatty acid-free BSA with or without the appropriate inhibitor before the addition of HDL. Five hours later, cells were pulsed with 0.2 mM [ $^{14}\text{C}$ ]oleate (Amersham Bioscience) for 2 h. Finally, cells were washed three times with buffer A and once with buffer A without BSA. The lipids were extracted twice from the cell monolayer and separated by TLC (SilicaGel G; Machery-Nagel, Dueren, Germany) (30). Cholesteryl esters formed were analyzed by scintillation counting. Cell proteins were dissolved in 0.1 N NaOH, and the protein was quantitated using the Bradford reagent (Bio-Rad).

### Confocal microscopy

Cells were seeded on coverslips and grown in the appropriate medium for 2 days. Then, the medium was switched to medium A with 5% human lipoprotein-deficient serum for cholesterol depletion. The next day, cells were kept in medium A with 2 mg/ml fatty acid-free BSA and incubated with the indicated amounts of Alexa-647 HDL for 1 h at  $37^\circ\text{C}$ . Afterward, a displacement and chase procedure was performed. Finally, the cells were fixed

with 4% paraformaldehyde (Sigma) in PBS for 20 min at room temperature, and nuclear staining was performed using 4',6-diamino-phenylindole (1  $\mu\text{g}/\text{ml}$ ; Sigma) for 5 min at room temperature. After washing, coverslips were mounted with Mowiol (Calbiochem). Samples were visualized on a Zeiss Axiovert 200 confocal microscope (Zeiss, Jena, Germany). Pictures were taken and analyzed using the imaging software LSM 500 (Zeiss).

### Statistics

The results are expressed as means  $\pm$  SD of three to five experiments.

## RESULTS

### HDL retroendocytosis proceeds unaltered in NPC fibroblast cells

Recently, we showed that HDL retroendocytosis still occurred when cholesterol transport from the lysosome to the ER was blocked by chloroquine (2), as demonstrated by a lack of stimulation of esterification when HDL was added (15). CHO cells overexpressing SR-BI but lacking the LDL receptor (ldla7-SRBI cells), incubated with 10  $\mu\text{g}/\text{ml}$   $^{125}\text{I}$ -HDL and with and without pretreatment of 50  $\mu\text{M}$  chloroquine for 15 min, showed all parts of HDL retroendocytosis (2). Chloroquine did not inhibit selective cholesteryl ester uptake mediated by SR-BI and only slightly decreased cholesterol efflux to HDL as an external acceptor (2). Furthermore, after trace labeling the cholesterol pool of ldla7-SRBI cells with [ $^3\text{H}$ ]cholesterol, cells pretreated with 50  $\mu\text{M}$  chloroquine and incubated with 10  $\mu\text{g}/\text{ml}$   $^{125}\text{I}$ -HDL exhibited cholesterol efflux mediated by HDL resecretion (data not shown). These data indicate that endocytosed HDL might not interact with lysosomes. Therefore, we hypothesized that HDL resecretion could mediate cholesterol efflux when cholesterol transport out of the lysosome is impaired.

To answer this, we used NPC patient fibroblast cells exhibiting a cholesterol uptake defect in which LDL-derived cholesterol is trapped in an endosomal/lysosomal compartment. First, control fibroblast cells showed all components of HDL retroendocytosis (Fig. 1, left). Second, NPC fibroblast cells also showed all parts of the HDL retroendocytosis pathway and to a similar degree as control fibroblast cells (Fig. 1, right). Approximately 40% of the HDL associated with the NPC cells was taken up (Fig. 1, right, black bar). Furthermore, approximately half of the HDL internalized was resecreted during the 30 min chase period (Fig. 1, right, striped bar). To exclude the possibility that the decrease of  $^{125}\text{I}$ -HDL seen during displacement and chase is attributable to HDL degradation, we measured HDL degradation in all media; as expected for fibroblast, almost no HDL degradation occurred (data not shown). Thus, fibroblast cells, including patient-derived NPC fibroblast cells, show all components of HDL uptake and resecretion.

To substantiate the finding of an undisturbed HDL uptake and resecretion pathway in NPC fibroblast cells, we used confocal microscopy imaging. The ldla7-SRBI cells were used as a control. Cells were incubated with 1  $\mu\text{g}/\text{ml}$



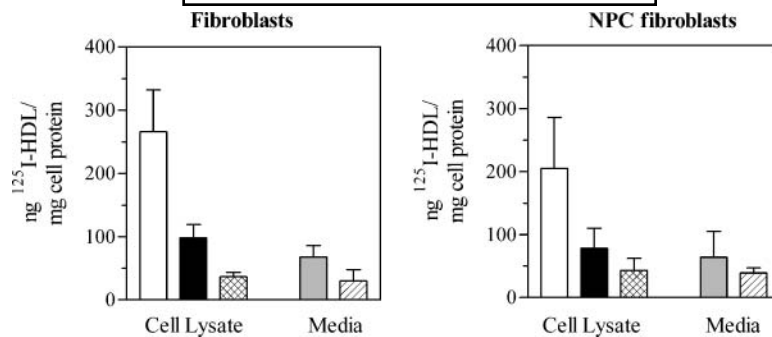


**Fig. 1.** HDL retroendocytosis in control (left) and Niemann-Pick type C (NPC) (right) fibroblast cells. Cells were incubated for 1 h with 10  $\mu\text{g}/\text{ml}$   $^{125}\text{I}$ -HDL, and association was measured as described in Methods (white bars). Then, cells were further incubated at 0°C for 2 h with a 100-fold excess of unlabeled HDL, which results in the displacement of  $^{125}\text{I}$ -HDL bound to the outside of the cell. The remaining  $^{125}\text{I}$  in the lysate is HDL that has been taken up by the cells (black bars). Finally, cells were further incubated at 37°C for 30 min with a 20-fold excess of HDL to allow efflux of the particle. The  $^{125}\text{I}$ -HDL remaining in the cell is shown (cross-hatched bars).  $^{125}\text{I}$ -HDL particles released to the medium during the 0°C displacement procedure (gray bars) and resecreted  $^{125}\text{I}$ -HDL particles to the medium after the chase (hatched bars) are shown. Data represent means  $\pm$  SD of four experiments.

Alexa-647 HDL for 1 h. This was followed by a displacement procedure at 0°C to remove cell surface-bound HDL. An intracellular accumulation of Alexa-647 HDL particles (red), especially in the perinuclear area, can be seen (Fig. 2, upper left). After rewarming, a parallel set of cells were incubated with unlabeled HDL to induce HDL resecretion. After 30 min, overall intracellular fluorescence representing HDL was diminished, with most of the remaining HDL located at the periphery of the cells (Fig. 2, upper right; see also supplementary movies I and II). These images indicated holo HDL particle uptake and resecretion in *ldla7-SRBI* cells.

In NPC fibroblast cells, HDL retroendocytosis was seen, but to a lesser extent (Fig. 2, lower). Intracellular HDL was detected after displacement (Fig. 2, lower left) and was reduced after the chase procedure (Fig. 2, lower right; see also supplementary movies III and IV). These data show that the HDL uptake pathway does not rely on the NPC1 protein. This is in contrast to the LDL receptor-mediated endocytosis pathway, in which LDL-derived cholesterol accumulates in late endosomes/lysosomes in NPC1-defective cells (31, 32).

#### HDL resecretion mediates [ $^3\text{H}$ ]cholesterol efflux when cholesterol transport out of lysosomes is blocked as a result of NPC1 ablation

After having established that HDL retroendocytosis proceeds in a patient-derived NPC fibroblast cell line, we analyzed whether HDL retroendocytosis can mediate [ $^3\text{H}$ ]cholesterol efflux in these patient cells. To assess whether retroendocytosis mediates cholesterol efflux in fibroblast cells, we preincubated the cells with 2  $\mu\text{Ci}$  of [ $^3\text{H}$ ]cholesterol overnight to trace-label the cellular cholesterol pool. The next day,  $^{125}\text{I}$ -HDL resecretion was analyzed. In parallel, [ $^3\text{H}$ ]cholesterol distribution between the cell lysate and the medium was assessed (Fig. 3). Control fibroblasts exhibited [ $^3\text{H}$ ]cholesterol efflux via HDL resecretion, as one-fourth of the cellular [ $^3\text{H}$ ]cho-

lesterol, or  $1.3 \pm 0.1$  pmol [ $^3\text{H}$ ]cholesterol/mg cell protein, was found in the medium after the 30 min chase (Fig. 3, left, gray bar). In NPC fibroblast cells, this [ $^3\text{H}$ ]cholesterol efflux was even higher (Fig. 3, right), as NPC fibroblast cells exhibited a higher initial [ $^3\text{H}$ ]cholesterol loading, consistent with the defect in cholesterol transport. Their [ $^3\text{H}$ ]cholesterol content was three times higher compared with control fibroblast cells. Cholesterol efflux was  $2.2 \pm 1.1$  pmol [ $^3\text{H}$ ]cholesterol/mg cell protein, with  $15 \pm 11$  pmol [ $^3\text{H}$ ]cholesterol/mg cell protein remaining in the cell lysate after the 0.5 h chase period (Fig. 3, right, gray bars). However, if we analyze the data as a percentage of the initial load of [ $^3\text{H}$ ]cholesterol, only  $13 \pm 6\%$  of the [ $^3\text{H}$ ]cholesterol was found in the medium, whereas in control fibroblasts  $21 \pm 2\%$  was detected.

Although HDL resecretion was similar between control and NPC fibroblasts, [ $^3\text{H}$ ]cholesterol was decreased significantly in NPC fibroblasts when expressed as a percentage ( $P < 0.05$ ,  $n = 4$ ). To determine whether the observed [ $^3\text{H}$ ]cholesterol efflux in NPC fibroblasts relies on HDL particle retroendocytosis, efflux was measured while blocking HDL particle uptake by 0°C incubation. An initial 0°C association was followed by 0°C displacement, but again, a 37°C chase with a 20-fold excess of unlabeled HDL was performed. This procedure reduced HDL resecretion to  $\sim 10\%$ . Similarly, cholesterol efflux was reduced. To exclude the possibility that the cholesterol efflux during the chase period is mediated by the unlabeled HDL added to the chase medium, a chase without a 20-fold excess of HDL was performed. Still, HDL resecretion and cholesterol efflux occurred to a similar, although somewhat lower, extent (data not shown). Together, these experiments indicate that the [ $^3\text{H}$ ]cholesterol efflux measured in our experimental setup is mediated by HDL resecretion and not by the external HDL present in the chase medium. Furthermore, the [ $^3\text{H}$ ]cholesterol as well as the protein moiety were TCA-precipitable in all media of the retroendocytosis experiment; after TCA precipita-

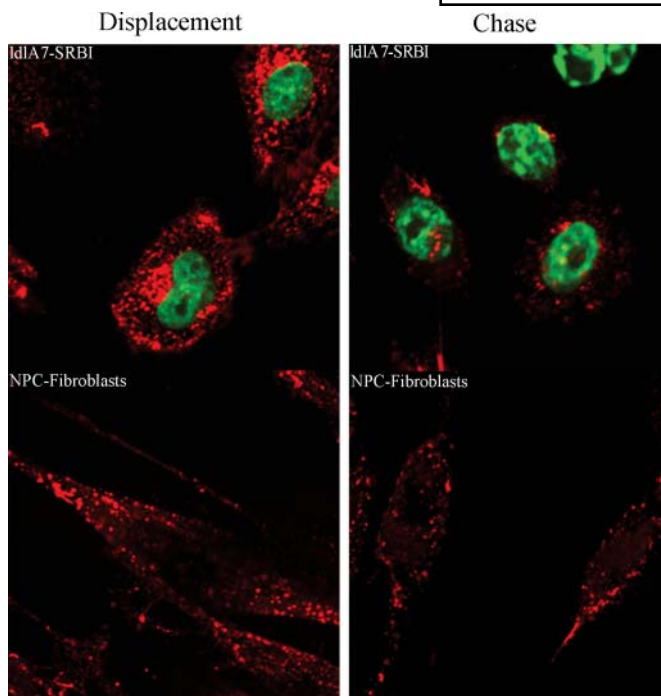


**Fig. 2.** Distribution of Alexa-647 HDL (red) during displacement and chase in ldlA7-SRBI cells (upper panels) and NPC fibroblast cells (lower panels). Cells were seeded on coverslips and grown, and cholesterol was depleted as described in Methods. ldlA7-SRBI and NPC fibroblast cells were incubated for 1 h at 37°C with 1 or 10  $\mu\text{g/ml}$  Alexa-647 HDL, respectively, followed by a displacement and chase procedure as stated in Methods. Finally, cells were fixed and counterstained with 4',6-diamino-phenylindole (green) for ldlA7-SRBI cells, and images were taken with a confocal microscope (Axiovert 200; Zeiss). After cell surface-bound HDL is removed using the displacement procedure, the remaining HDL is located intracellularly, which is seen for both cell types (left panels; see also supplementary movies I and III). Intracellularly located HDL is further recycled out of the cells during a 30 min chase period. A markedly decreased Alexa-647 HDL signal as well as HDL particles located mainly at the inner or outer leaflet of the cell membrane can be detected (right panels; see also supplementary movies II and IV). All images were obtained by implementing z-scanning, and images presented represent a center layer of the cells. The data were reconstructed to obtain three-dimensional images of the scanned cells and can be seen as supplementary movies I–IV.

tion, almost no counts were detected in the supernatant. Thus, HDL retroendocytosis can mediate cholesterol efflux when intracellular cholesterol trafficking is altered because of a defect in the NPC1 gene.

#### HDL resecretion mediates cholesterol efflux when cholesterol transport out of lysosomes is blocked by inhibitors

To substantiate these data, three inhibitors blocking intracellular cholesterol transport were chosen: imipramine, U18666A, and monensin. Imipramine and U18666A block cholesterol transport out of the lysosome; monensin, a Golgi-perturbing agent, blocks vesicle secretion and inhibits the endocytosis of LDL. To confirm the proposed functions of these inhibitors, we tested their ability to block cholesterol esterification by ACAT. Therefore, ldlA7-SRBI

cells were incubated with increasing concentrations of imipramine, monensin, or U18666A for 15 min and then for 5 h with 100  $\mu\text{g/ml}$  HDL. Finally, cholesterol esterification was induced by adding 0.2 mM [ $^{14}\text{C}$ ]oleate for an additional 2 h. Stimulation of esterification was measured as the formation of cholesteryl [ $^{14}\text{C}$ ]oleate. Like chloroquine (15), imipramine (50  $\mu\text{M}$ ), U18666A (50  $\mu\text{M}$ ), and monensin (50  $\mu\text{M}$ ) inhibited HDL-mediated stimulation of cholesterol esterification significantly, from  $\sim 3,000$  pmol cholesteryl [ $^{14}\text{C}$ ]oleate/mg cell protein to  $\sim 20\%$  (data not shown), whereas the stimulation by 25-hydroxycholesterol, a substance that freely passes the membrane, was almost unaltered (data not shown). This indicates that the delivery of cholesterol derived from HDL to the ER is blocked by these substances but the ACAT enzyme is not inhibited directly.

To test HDL retroendocytosis in the presence of these inhibitors, ldlA7-SRBI cells were first incubated with 50  $\mu\text{M}$  imipramine for 15 min before the addition of [ $^{125}\text{I}$ ]HDL. After removal of the inhibitor, HDL uptake and resecretion were followed (Fig. 4, upper, second panel). HDL retroendocytosis did not differ significantly from that in untreated cells (Fig. 4, upper left panel). Second, cells were preincubated with 50  $\mu\text{M}$  U18666A, leading to a similar uptake and resecretion pattern (Fig. 4, upper third panel). Finally, cells treated with 50  $\mu\text{M}$  monensin exhibited lower displacement and resecretion of HDL (Fig. 4, upper right panel). Thus, although these substances blocked cholesterol delivery to the ER, HDL uptake and resecretion were still proceeding, leading to the question of whether [ $^3\text{H}$ ]cholesterol efflux mediated by HDL resecretion also occurs after inhibitor treatment. Therefore, ldlA7-SRBI cells were trace-labeled with [ $^3\text{H}$ ]cholesterol on the day before the experiment. Association, displacement, and chase experiments were performed by preincubating cells with one of the inhibitors. Figure 4 (lower) shows the [ $^{125}\text{I}$ ] (open bars) and [ $^3\text{H}$ ] (gray bars) contents of the lysate and medium after the chase. Like control cells (lower left panel;  $13.6 \pm 3.0$  pmol [ $^3\text{H}$ ]cholesterol/mg cell protein,  $n = 4$ ), imipramine-treated cells (lower second panel;  $3.5 \pm 2.4$  pmol [ $^3\text{H}$ ]cholesterol/mg cell protein,  $n = 4$ ), U18666A-treated cells (lower third panel;  $5.0 \pm 1.0$  pmol [ $^3\text{H}$ ]cholesterol/mg cell protein,  $n = 4$ ), and monensin-treated cells (right panels;  $4.5 \pm 1.5$  pmol [ $^3\text{H}$ ]cholesterol/mg cell protein,  $n = 3$ ) showed somewhat lower [ $^3\text{H}$ ]cholesterol efflux during the 30 min chase period. When we analyzed the data as percentages of initial loading, all three inhibitors showed significant decreases in [ $^3\text{H}$ ]cholesterol efflux, from 21% in control cells to  $\sim 10\%$  in inhibitor-treated cells ( $P < 0.05$ ,  $n = 3$ ). Therefore, resecretion-mediated cholesterol efflux was lower in treated cells than in control cells but occurred while intracellular cholesterol transport was blocked.

#### HDL retroendocytosis occurs in two mutant CHO cell lines

CHO 2-2 cells, a CHO cell line with a defect in intracellular LDL cholesterol transfer, was used (33). The CHO 2-2 cell line, established by Dahl et al. (34, 35) using

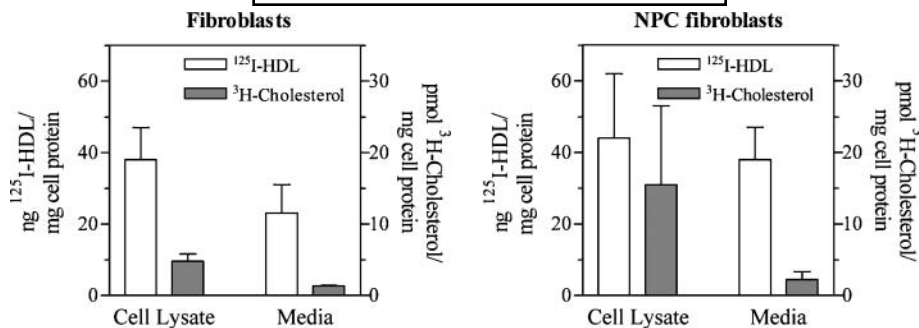


**Fig. 3.** Cholesterol efflux mediated by HDL particle resecretion in control (left) and NPC fibroblast (right) cells. Before the experiment, cells were trace-labeled with 2  $\mu\text{Ci}$  of [ $^3\text{H}$ ]cholesterol per well for 24 h. On the experimental day, cells were incubated with 10  $\mu\text{g}/\text{ml}$   $^{125}\text{I}$ -HDL for 1 h, followed by incubation at  $0^\circ\text{C}$  for 2 h with a 100-fold excess of HDL and a final incubation with a 20-fold excess of HDL at  $37^\circ\text{C}$  for 30 min. Then, after medium was collected, cells were lysed and aliquots were analyzed for their  $^3\text{H}$  (gray bars) and  $^{125}\text{I}$  (white bars) contents. Data represent means  $\pm$  SD of four experiments. Note that cholesterol efflux mediated via HDL resecretion occurs in NPC fibroblast cells.

amphotericin B treatment, exhibits a NPC phenotype (33). Furthermore, a second CHO cell line with a defect in intracellular cholesterol transport, the CHO 3-6 cell line, was used. CHO 3-6 cells are profoundly defective in LDL cholesterol transport to the ER but exhibit nearly normal movement of LDL cholesterol from the lysosome to the plasma membrane (35). First, HDL uptake and resecretion were investigated in these cell lines. CHO 2-2 and 3-6 cells showed all parts of HDL retroendocytosis (Fig. 5). SR-BI overexpression led to increases in HDL association, uptake, and resecretion (Fig. 5, right). This SR-BI dependence was expected, as overexpression of SR-BI in another CHO cell line (IdIA7 cells) resulted in an increase in HDL retroendocytosis, as reported earlier (2).

### Overall characterization of cholesterol uptake in mutant CHO cell lines

To characterize the CHO 2-2 cell line in terms of its cholesterol mobilization, we analyzed its cholesterol uptake behavior to HDL with special emphasis on alterations induced by SR-BI overexpression. CHO 2-2 cells exhibited a similar stimulation of cholesterol esterification as IdIA7 cells after HDL incubation (Fig. 6, compare open circles in left and right panels). In IdIA7 cells, SR-BI overexpression led to an enormous dose-dependent increase in cholesteryl [ $^{14}\text{C}$ ]oleate (Fig. 6, right, closed triangles), whereas CHO 2-2 SRBI cells showed only a modest response (Fig. 6, left, closed triangles). The absence of the induction of cholesterol esterification was not attributable to a defect in the

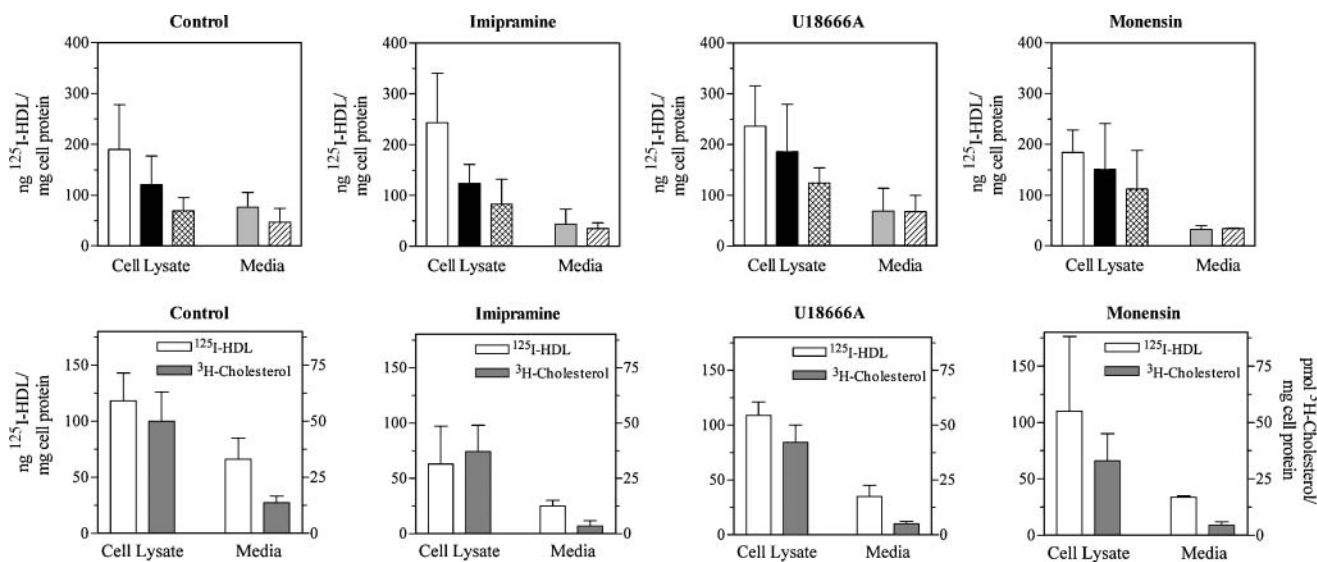


**Fig. 4.** Inhibitor treatment does not influence HDL resecretion-mediated cholesterol efflux. HDL retroendocytosis (upper panels) and cholesterol efflux mediated by HDL particle resecretion (lower panels) in IdIA7-SRBI cells treated with imipramine (50  $\mu\text{M}$ ), U18666A (50  $\mu\text{M}$ ), or monensin (50  $\mu\text{M}$ ) are shown. Cells were prepared and analyzed as described above, and bars in the upper and lower panels are as described for Figs. 1 and 3, respectively. Means  $\pm$  SD of four experiments are depicted. Note that cholesterol efflux mediated via HDL resecretion occurs after inhibitor treatment.



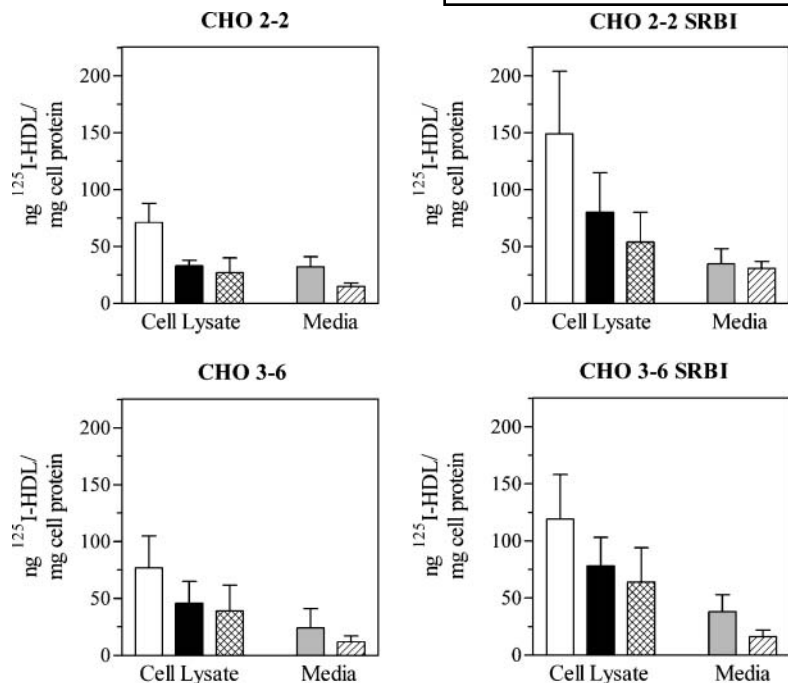


**Fig. 5.** HDL retroendocytosis in CHO 2-2 (upper left), CHO 2-2 SRBI (upper right), CHO 3-6 (lower left), and CHO 3-6 SRBI (lower right) cells. Cells were incubated for 1 h with 10  $\mu\text{g}/\text{ml}$   $^{125}\text{I}$ -HDL, and association was measured as described in Methods. Then, a subset of cells was incubated at 0°C for 2 h with a 100-fold excess of unlabeled HDL, and cells were finally incubated at 37°C for 30 min with a 20 $\times$  excess of HDL. Cell association (white bars), HDL uptake (black bars), and intracellular HDL remaining in the cell lysate after the chase (cross-hatched bars) are shown.  $^{125}\text{I}$ -HDL particles released to the medium during displacement are presented (gray bars). Resecreted  $^{125}\text{I}$ -HDL particles to the medium after the chase are displayed (hatched bars). Means  $\pm$  SD of four experiments are depicted. Note that HDL uptake and rescretion are higher with scavenger receptor class B type I (SR-BI) overexpression.

ACAT enzyme by itself, as both CHO 2-2 and CHO 2-2 SRBI cells reached similar levels of 25-hydroxycholesterol-induced stimulation of esterification as did control IdIA7 or IdIA7-SRBI cells (data not shown). The small amount of stimulation of cholesterol esterification in the CHO 2-2 and CHO 2-2 SRBI cells was completely blocked by chloroquine as well as by imipramine and U18666A (data not shown). LDL did not stimulate cholesterol esterification, confirming that these cells have a block in the LDL uptake pathway (data not shown). Using the CHO 3-6 cells, again there was only a slight stimulation of cholesterol esterification after HDL incubation, even with SR-BI overexpression (Fig. 6, middle panel). The absence of the induction of cholesterol esterification was not the result of a defect in the ACAT enzyme, as both CHO 3-6 and CHO3-6 SRBI cells showed similar levels of 25-hydroxycholesterol-induced stimulation of esterification compared with CHO 2-2 and also IdIA7 cells (data not shown). These data indicate that cholesterol taken up by selective uptake via

SR-BI uses a transport route to the ER via the lysosomal/endosomal pathway.

#### HDL resecretion mediates cholesterol efflux in the CHO 2-2 and 3-6 cell lines in a SR-BI-dependent manner

Next, we assessed whether the CHO 2-2 cells exhibit cholesterol efflux mediated by HDL resecretion (Fig. 7). Indeed, HDL resecretion did mediate cholesterol efflux (Fig. 7, left, gray bars), as  $3.3 \pm 1$  pmol [ $^3\text{H}$ ]cholesterol/mg cell protein was found in the medium after the 30 min chase period. Overexpression of SR-BI resulted in an increase in resecreted HDL (Fig. 7, right, white bars). This increased HDL resecretion was followed by an increase in cholesterol efflux to the medium. In CHO 2-2 cells overexpressing SR-BI,  $5.3 \pm 0.8$  pmol [ $^3\text{H}$ ]cholesterol/mg cell protein was found in the medium after the 30 min chase period (Fig. 7, right, gray bars). CHO 3-6 cells also showed cholesterol efflux mediated by HDL retroendocytosis (Fig. 7, left;  $2.7 \pm 0.8$  pmol [ $^3\text{H}$ ]cholesterol/mg cell pro-

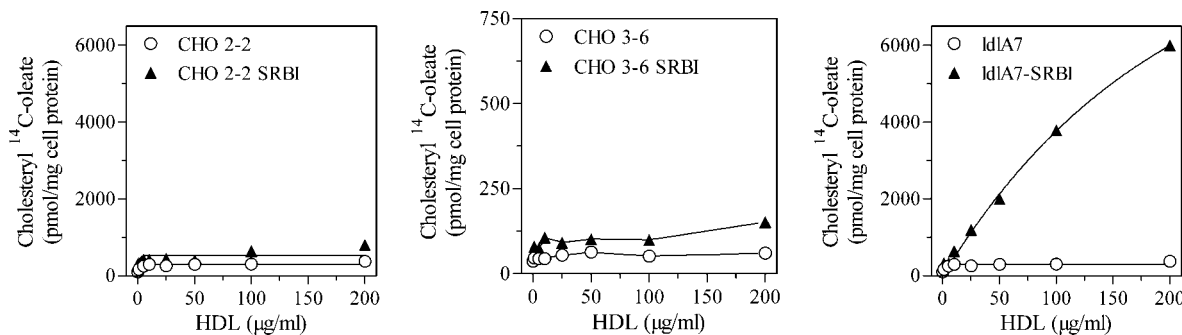


**Fig. 6.** Stimulation of cholesteryl [ $^{14}\text{C}$ ]oleate formation by HDL in CHO 2-2 and CHO 2-2 SRBI cells (left panel), CHO 3-6 and CHO 3-6 SRBI cells (middle panel), and IdIA7 and IdIA7-SRBI cells (right panel). Cells were incubated with increasing concentrations of HDL for 5 h. Then, 0.2 mM [ $^{14}\text{C}$ ]oleate was added to the medium for 2 h. Cellular cholesteryl ester formation was analyzed by TLC. Data points represent means of triplicate values. The experiment was repeated giving similar results.

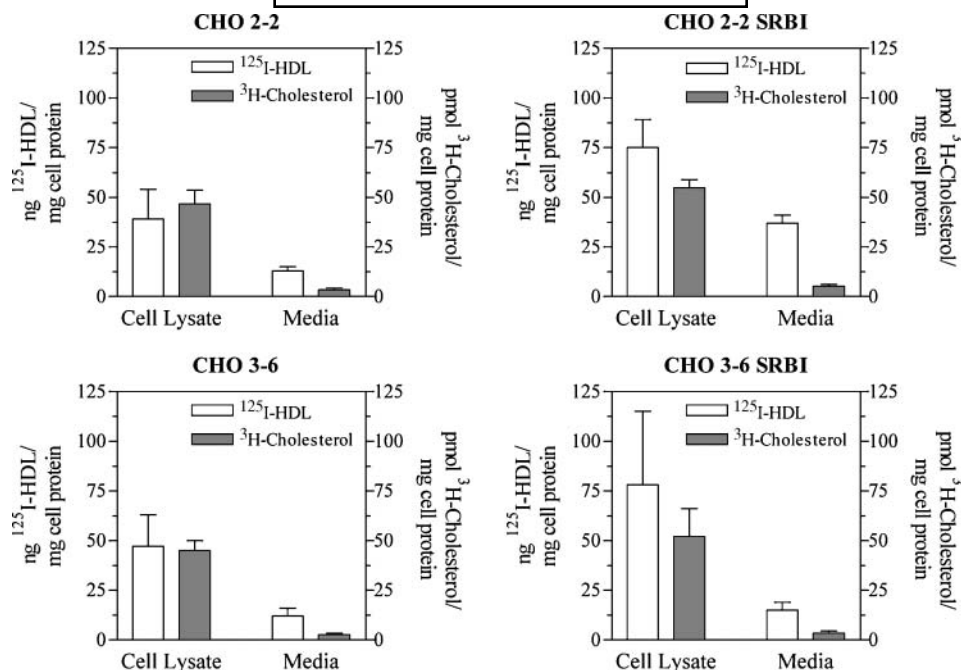


**Fig. 7.** Cholesterol efflux mediated by HDL particle resecretion in CHO 2-2 cells (upper left) and CHO 2-2 SRBI cells (upper right) and in CHO 3-6 cells (lower left) and CHO 3-6 SRBI cells (lower right). Before the experiment, cells were trace-labeled with [ $^3\text{H}$ ]cholesterol for 24 h. On the experimental day, cells were incubated with 10  $\mu\text{g}/\text{ml}$   $^{125}\text{I}$ -HDL for 1 h, followed by incubation at 0°C for 2 h with a 100-fold excess of HDL and a final incubation with a 20-fold excess of HDL at 37°C for 30 min. Then, the medium was collected, cells were lysed, and aliquots were analyzed for their  $^3\text{H}$  (gray bars) and  $^{125}\text{I}$  (white bars) contents. Means  $\pm$  SD of three experiments are depicted. Note that cholesterol efflux mediated via HDL resecretion is somewhat higher after SR-BI overexpression.

tein). Again, cholesterol efflux mediated by HDL retroendocytosis was stimulated by SR-BI overexpression, although to a lesser extent (Fig. 7, right;  $3.4 \pm 1.0$  pmol [ $^3\text{H}$ ]cholesterol/mg cell protein). These data demonstrate that HDL resecretion and concomitant cholesterol efflux occur. Thus, this pathway is not connected to receptor-mediated endocytosis facilitated by the LDL receptor and is independent of cholesterol mobilization from the lysosome.

## DISCUSSION

The current study was designed to analyze the role of HDL uptake and resecretion for cholesterol homeostasis in cases of disturbed intracellular cholesterol trafficking. We hypothesized that HDL retroendocytosis might be important for the fine-tuning of cholesterol export. To test this hypothesis, we applied the following: 1) inhibitors of the intracellular cholesterol transport: chloroquine, imipramine, monensin, and U18666A did not substantially alter HDL resecretion but resulted in a somewhat lower cholesterol flux mediated by retroendocytosis; 2) two somatic CHO cell lines, both displaying a transport defect in intracellular cholesterol transfer to the ER or plasma membrane (CHO 2-2 and 3-6 cells), exhibited all parts of the HDL retroendocytosis pathway, with even a slight enhancement in cholesterol efflux via HDL resecretion;

and 3) patient fibroblast cells from a genetic disorder of cholesterol metabolism in receptor-mediated endocytosis of LDL (namely, NPC disease), which showed normal HDL uptake and resecretion compared with control fibroblast cells. The NPC fibroblast cells still exhibited [ $^3\text{H}$ ]cholesterol efflux via HDL resecretion. Thus, we have shown that HDL retroendocytosis still is functional in cases in which LDL receptor-mediated endocytosis is blocked at the lysosomal stage. HDL resecretion may present an alternative pathway to remove excess intracellular cholesterol and may be important in cells with defects in a part of the cholesterol exchange pathway. Thus, HDL retroendocytosis could be responsible for maintaining or balancing at least in part their cholesterol homeostasis.

In this study, we demonstrated that lysosomes are not a way station of endocytosed HDL by applying several inhibitors that block cholesterol transport out of the lysosome. It is known that several vesicular endosomal transport pathways can substitute for each other. Therefore, there is still the possibility that HDL takes a similar uptake route as LDL but then diverges. One has to consider that perturbation of the membrane traffic in NPC fibroblasts occurs primarily in the late endocytic pathway (36–38), as shown by the abnormal late endosomal/lysosomal accumulation of cholesterol, which is normally targeted to the cell surface and the ER. Furthermore, mutations in NPC1 do not exclusively affect cholesterol




transport but target vesicle-mediated transport pathways that affect a wide range of endocytosed cargo (36, 39). As HDL retroendocytosis occurs in NPC1 fibroblasts, the HDL particles en route to the perinuclear area, possibly via the endosomal recycling compartment, use an alternative vesicle-mediated transport pathway or diverge earlier in the endocytic process.

Interestingly, the mutant CHO cell lines as well as NPC fibroblast cells exhibited higher intracellular levels of [<sup>3</sup>H]cholesterol after overnight incubation than control cells. This finding is consistent with their disorders in cholesterol metabolism, as all of these cell systems are reported to accumulate cholesterol intracellularly. One can speculate that this overall higher cholesterol content results in the observed increased release of [<sup>3</sup>H]cholesterol by HDL retroendocytosis.

Several ways of cholesterol transfer from cells to HDL seem possible. Cholesterol transfer from cells to internalized HDL may be mediated through aqueous diffusion along a concentration gradient or by transfer between HDL and membranes of endosomal compartments or lipid droplets. Indeed, HDL was reported to be located in close proximity to lipid droplets in macrophages (5). Recently, Cheruku et al. (40) showed, using small unilamellar vesicles, that the rate of cholesterol transfer, mediated by NPC2, increased in proportion to the acceptor vesicle concentration. When using anionic phospholipids as acceptor vesicles, cholesterol transfer was even enhanced (40). The authors proposed that the delivery of cholesterol through NPC2 is mediated via direct protein-membrane collision (40). HDL represents a protein-coated phospholipid vesicle; therefore, this "collisional transfer" could be a way by which endocytosed HDL is filled with intracellular cholesterol. As HDL retroendocytosis-mediated cholesterol efflux was not impaired in patient fibroblast cells carrying a defect in the NPC1 gene, the proposed collisional transfer mechanism cannot be facilitated by the NPC1 protein alone; however, other proteins, like NPC2, may play a role in the described efflux pathway.

The new cholesterol efflux pathway via HDL resecrection described here was functional in mutant CHO 2-2 cells, representing an NPC phenotype, and in another phenotype, CHO 3-6, accumulating intracellular cholesterol (Fig. 7). CHO 2-2 and CHO 3-6 cells transferred 3.3 and 2.7 pmol cholesterol/mg cell protein/30 min, respectively. Interestingly, there was even a slight increase in this cholesterol efflux when SR-BI expression was induced in these cells (5.3 and 3.4 pmol cholesterol/mg cell protein/30 min, respectively). Although NPC fibroblast cells exhibited ~13% cholesterol efflux, the mutant cell lines showed only half of this efflux. In addition, the data showed that CHO 2-2 cells with a defect in mobilizing plasma membrane cholesterol could bypass this defect using cholesterol efflux mediated by HDL resecrection. Next, both inhibitor treatment and the NPC phenotype resulted in a decrease of [<sup>3</sup>H]cholesterol efflux to ~50% of the corresponding control. These data show that there is a disconnection between HDL resecrection and [<sup>3</sup>H]cholesterol efflux under these circumstances.

One of the currently most discussed receptors mediating cholesterol efflux to HDL, the ABC transport family, is not likely to be involved in cholesterol efflux from NPC fibroblasts. Cholesterol efflux to the physiological acceptor apoA-I proceeded more rapidly in wild-type CHO cells than in CT60 cells, CHO cells carrying the NPC mutation (41). Recent studies showed that apoA-I exhibited diminished ability to mobilize cholesterol in NPC1-negative human fibroblasts, as a result of the diminished basal and cholesterol-stimulated levels of ABCA1 mRNA and protein in these cells (13). Next, it was demonstrated that in ongoing neurodegeneration, none of the target genes of the liver X receptor was activated in the cerebellum of NPC<sup>-/-</sup> mice, including ABCA1 and ABCG1 (42). ABCG1 was reported to mediate cholesterol efflux to mature HDL (43, 44). However, ABCA1 and ABCG1 receptors seem to be not functional, at least in the brain of NPC animals. Recently, Boadu et al. (45) demonstrated in NPC fibroblasts that treatment with liver X receptor agonists restored ABCA1- and ABCG1-mediated cholesterol efflux. This shows that the main consequence of the NPC phenotype is a depletion of liver X receptor ligands, resulting in a downregulation of cholesterol efflux pathways. In patients with cholesterol-trafficking defects, HDL retroendocytosis could play a role for cholesterol efflux, as NPC patients exhibit no vascular involvement leading to atherosclerosis (10). This indicates that alternative mechanisms must handle cholesterol efflux to maintain cholesterol transport to and from the periphery.

In summary, our study demonstrates that HDL retroendocytosis represents an alternative pathway of [<sup>3</sup>H]cholesterol removal for cells when cholesterol homeostasis is disturbed. This pathway could circumvent defects in cholesterol distribution occurring in diseases like NPC disease. 

The authors thank Melissa Hyatt for excellent technical assistance and Dr. Helen H. Hobbs for her support of this work. The SR-BI-overexpressing mutant CHO cell lines were established in the laboratory of Dr. Helen H. Hobbs (University of Texas Southwestern Medical Center, Dallas, TX). CHO 2-2 and CHO 3-6 cells were kindly provided by Dr. Laura Liscum (Tufts University, Boston, MA), and NPC fibroblasts were from Dr. Peter Pentchev (National Institutes of Health, Bethesda, MD). Confocal microscopy was performed at the Institute for Histology and Embryology, Veterinarian University of Vienna, with the help of Dr. Ingrid Walter. H.S. was supported by Austrian Science Foundation Grants P16362-B07 and P20116-B11.

## REFERENCES

1. Jessup, W., I. C. Gelissen, K. Gaus, and L. Kritharides. 2006. Roles of ATP binding cassette transporters A1 and G1, scavenger receptor BI and membrane lipid domains in cholesterol export from macrophages. *Curr. Opin. Lipidol.* **17**: 247–257.
2. Pagler, T. A., S. Rhode, A. Neuhofer, H. Laggner, W. Strobl, C. Hinterndorfer, I. Volf, M. Pavelka, E. R. Eckhardt, D. R. Van Der Westhuyzen, et al. 2006. SR-BI-mediated high density lipoprotein (HDL) endocytosis leads to HDL resecrection facilitating cholesterol efflux. *J. Biol. Chem.* **281**: 11193–11204.

3. Rhode, S., A. Breuer, J. Hesse, M. Sonnleitner, T. A. Pagler, M. Doring, G. J. Schutz, and H. Stangl. 2004. Visualization of the uptake of individual HDL particles in living cells via the scavenger receptor class B type I. *Cell Biochem. Biophys.* **41**: 343–356.
4. Bierman, E. L., O. Stein, and Y. Stein. 1974. Lipoprotein uptake and metabolism by rat aortic smooth muscle cells in tissue culture. *Circ. Res.* **35**: 136–150.
5. Schmitz, G., H. Robenek, U. Lohmann, and G. Assmann. 1985. Interaction of high density lipoproteins with cholesteryl ester-laden macrophages: biochemical and morphological characterization of cell surface receptor binding, endocytosis and rescretion of high density lipoproteins by macrophages. *EMBO J.* **4**: 613–622.
6. DeLamatre, J. G., T. G. Sarphe, R. C. Archibold, and C. A. Hornick. 1990. Metabolism of apoE-free high density lipoproteins in rat hepatoma cells: evidence for a retroendocytic pathway. *J. Lipid Res.* **31**: 191–202.
7. Silver, D. L., N. Wang, X. Xiao, and A. R. Tall. 2001. High density lipoprotein (HDL) particle uptake mediated by scavenger receptor class B type 1 results in selective sorting of HDL cholesterol from protein and polarized cholesterol secretion. *J. Biol. Chem.* **276**: 25287–25293.
8. Nieland, T. J., M. Ehrlich, M. Krieger, and T. Kirchhausen. 2005. Endocytosis is not required for the selective lipid uptake mediated by murine SR-BI. *Biochim. Biophys. Acta.* **1734**: 44–51.
9. Wustner, D., M. Mondal, A. Huang, and F. R. Maxfield. 2004. Different transport routes for high density lipoprotein and its associated free sterol in polarized hepatic cells. *J. Lipid Res.* **45**: 427–437.
10. Patterson, M. C., M. T. Vanier, K. Suzuki, J. A. Morris, E. Carstea, E. B. Neufeld, J. E. Blanchette-Mackie, and P. G. Pentchev. 2001. Niemann-Pick disease type C: a lipid trafficking disorder. In *The Metabolic and Molecular Bases of Inherited Diseases*. Vol. III. C. R. Scriver, A. L. Beaudet, W. S. Sly, and D. Valle, editors. McGraw-Hill, New York. 3611–3633.
11. Patterson, M. C. 2003. A riddle wrapped in a mystery: understanding Niemann-Pick disease, type C. *Neurologist.* **9**: 301–310.
12. Walkley, S. U. 2001. New proteins from old diseases provide novel insights in cell biology. *Curr. Opin. Neurol.* **14**: 805–810.
13. Choi, H. Y., B. Karten, T. Chan, J. E. Vance, W. L. Greer, R. A. Heidenreich, W. S. Garver, and G. A. Francis. 2003. Impaired ABCA1-dependent lipid efflux and hypoalphalipoproteinemia in human Niemann-Pick type C disease. *J. Biol. Chem.* **278**: 32569–32577.
14. Ji, Y., B. Jian, N. Wang, Y. Sun, M. L. Moya, M. C. Phillips, G. H. Rothblat, J. B. Swaney, and A. R. Tall. 1997. Scavenger receptor BI promotes high density lipoprotein-mediated cellular cholesterol efflux. *J. Biol. Chem.* **272**: 20982–20985.
15. Stangl, H., G. Cao, K. L. Wyne, and H. H. Hobbs. 1998. Scavenger receptor, class B, type I-dependent stimulation of cholesterol esterification by high density lipoproteins, low density lipoproteins, and nonlipoprotein cholesterol. *J. Biol. Chem.* **273**: 31002–31008.
16. Stangl, H., M. Hyatt, and H. H. Hobbs. 1999. Transport of lipids from high and low density lipoproteins via scavenger receptor-BI. *J. Biol. Chem.* **274**: 32692–32698.
17. Yancey, P. G., M. De La Llera-Moya, S. Swarnakar, P. Monzo, S. M. Klein, M. A. Connelly, W. J. Johnson, D. L. Williams, and G. H. Rothblat. 2000. High density lipoprotein phospholipid composition is a major determinant of the bi-directional flux and net movement of cellular free cholesterol mediated by scavenger receptor BI. *J. Biol. Chem.* **275**: 36596–36604.
18. Gu, X., K. Kozarsky, and M. Krieger. 2000. Scavenger receptor class B, type I-mediated [<sup>3</sup>H]cholesterol efflux to high and low density lipoproteins is dependent on lipoprotein binding to the receptor. *J. Biol. Chem.* **275**: 29993–30001.
19. Chroni, A., T. J. Nieland, K. E. Kypreos, M. Krieger, and V. I. Zannis. 2005. SR-BI mediates cholesterol efflux via its interactions with lipid-bound apoE. Structural mutations in SR-BI diminish cholesterol efflux. *Biochemistry.* **44**: 13132–13143.
20. Zannis, V. I., A. Chroni, and M. Krieger. 2006. Role of apoA-I, ABCA1, LCAT, and SR-BI in the biogenesis of HDL. *J. Mol. Med.* **84**: 276–294.
21. De Duve, C., T. De Barse, B. Poole, A. Trouet, P. Tulkens, and F. Van Hoof. 1974. Commentary. Lysosomotropic agents. *Biochem. Pharmacol.* **23**: 2495–2531.
22. Underwood, K. W., B. Andemariam, G. L. McWilliams, and L. Liscum. 1996. Quantitative analysis of hydrophobic amine inhibition of intracellular cholesterol transport. *J. Lipid Res.* **37**: 1556–1568.
23. Dinter, A., and E. G. Berger. 1998. Golgi-disturbing agents. *Histochem. Cell Biol.* **109**: 571–590.
24. Basu, S. K., J. L. Goldstein, R. G. Anderson, and M. S. Brown. 1981. Monensin interrupts the recycling of low density lipoprotein receptors in human fibroblasts. *Cell.* **24**: 493–502.
25. Tartakoff, A. M., and P. Vassalli. 1983. Lectin-binding sites as markers of Golgi subcompartments: proximal-to-distal maturation of oligosaccharides. *J. Cell Biol.* **97**: 1243–1248.
26. Tartakoff, A. M., and P. Vassalli. 1977. Plasma cell immunoglobulin secretion: arrest is accompanied by alterations of the Golgi complex. *J. Exp. Med.* **146**: 1332–1345.
27. Kingsley, D. M., and M. Krieger. 1984. Receptor-mediated endocytosis of low density lipoprotein: somatic cell mutants define multiple genes required for expression of surface-receptor activity. *Proc. Natl. Acad. Sci. USA.* **81**: 5454–5458.
28. Acton, S., A. Rigotti, K. T. Landschulz, S. Xu, H. H. Hobbs, and M. Krieger. 1996. Identification of scavenger receptor SR-BI as a high density lipoprotein receptor. *Science.* **271**: 518–520.
29. Schumaker, V. N., and D. L. Puppione. 1986. Sequential flotation ultracentrifugation. *Methods Enzymol.* **128**: 155–170.
30. Goldstein, J. L., S. K. Basu, and M. S. Brown. 1983. Receptor-mediated endocytosis of low-density lipoprotein in cultured cells. *Methods Enzymol.* **98**: 241–260.
31. Pentchev, P. G., M. E. Comly, H. S. Kruth, M. T. Vanier, D. A. Wenger, S. Patel, and R. O. Brady. 1985. A defect in cholesterol esterification in Niemann-Pick disease (type C) patients. *Proc. Natl. Acad. Sci. USA.* **82**: 8247–8251.
32. Pentchev, P. G., M. E. Comly, H. S. Kruth, T. Tokoro, J. Butler, J. Sokol, M. Filling-Katz, J. M. Quirk, D. C. Marshall, S. Patel, et al. 1987. Group C Niemann-Pick disease: faulty regulation of low density lipoprotein uptake and cholesterol storage in cultured fibroblasts. *FASEB J.* **1**: 40–45.
33. Underwood, K. W., N. L. Jacobs, A. Howley, and L. Liscum. 1998. Evidence for a cholesterol transport pathway from lysosomes to endoplasmic reticulum that is independent of the plasma membrane. *J. Biol. Chem.* **273**: 4266–4274.
34. Dahl, N. K., K. L. Reed, M. A. Daunais, J. R. Faust, and L. Liscum. 1992. Isolation and characterization of Chinese hamster ovary cells defective in the intracellular metabolism of low density lipoprotein-derived cholesterol. *J. Biol. Chem.* **267**: 4889–4896.
35. Dahl, N. K., M. A. Daunais, and L. Liscum. 1994. A second complementation class of cholesterol transport mutants with a variant Niemann-Pick type C phenotype. *J. Lipid Res.* **35**: 1839–1849.
36. Neufeld, E. B., M. Wastney, S. Patel, S. Suresh, A. M. Cooney, N. K. Dwyer, C. F. Roff, K. Ohno, J. A. Morris, E. D. Carstea, et al. 1999. The Niemann-Pick C1 protein resides in a vesicular compartment linked to retrograde transport of multiple lysosomal cargo. *J. Biol. Chem.* **274**: 9627–9635.
37. Lange, Y., J. Ye, M. Rigney, and T. Steck. 2000. Cholesterol movement in Niemann-Pick type C cells and in cells treated with amphiphiles. *J. Biol. Chem.* **275**: 17468–17475.
38. Cruz, J. C., S. Sugii, C. Yu, and T. Y. Chang. 2000. Role of Niemann-Pick type C1 protein in intracellular trafficking of low density lipoprotein-derived cholesterol. *J. Biol. Chem.* **275**: 4013–4021.
39. Vance, J. E. 2006. Lipid imbalance in the neurological disorder, Niemann-Pick C disease. *FEBS Lett.* **580**: 5518–5524.
40. Cheruku, S. R., Z. Xu, R. Dutia, P. Lobel, and J. Storch. 2006. Mechanism of cholesterol transfer from the Niemann-Pick type C2 protein to model membranes supports a role in lysosomal cholesterol transport. *J. Biol. Chem.* **281**: 31594–31604.
41. Lusa, S., T. S. Blom, E. L. Eskelinen, E. Kuusmanen, J. E. Mansson, K. Simons, and E. Ikonen. 2001. Depletion of rafts in late endocytic membranes is controlled by NPC1-dependent recycling of cholesterol to the plasma membrane. *J. Cell Sci.* **114**: 1893–1900.
42. Li, H., J. J. Repa, M. A. Valasek, E. P. Beltroy, S. D. Turley, D. C. German, and J. M. Dietschy. 2005. Molecular, anatomical, and biochemical events associated with neurodegeneration in mice with Niemann-Pick type C disease. *J. Neuropathol. Exp. Neurol.* **64**: 323–333.
43. Gelissen, I. C., M. Harris, K. A. Rye, C. Quinn, A. J. Brown, M. Kockx, S. Cartland, M. Packianathan, L. Kritharides, and W. Jessup. 2006. ABCA1 and ABCG1 synergize to mediate cholesterol export to apoA-I. *Arterioscler. Thromb. Vasc. Biol.* **26**: 534–540.
44. Vaughan, A. M., and J. F. Oram. 2006. ABCA1 and ABCG1 or ABCG4 act sequentially to remove cellular cholesterol and generate cholesterol-rich HDL. *J. Lipid Res.* **47**: 2433–2443.
45. Boadu, E., H. Y. Choi, D. W. Lee, E. I. Waddington, T. Chan, B. Asztalos, J. E. Vance, A. Chan, G. Castro, and G. A. Francis. 2006. Correction of apolipoprotein A-I-mediated lipid efflux and high density lipoprotein particle formation in human Niemann-Pick type C disease fibroblasts. *J. Biol. Chem.* **281**: 37081–37090.